The determination of the post-Newtonian parameter γ during the cruise phase of BepiColombo

Luigi Imperi[1] **and Luciano Iess**[1]

[1] Department of Mechanical and Aerospace Engineering, Sapienza University of Rome, Rome, Italy

E-mail: luigi.imperi@uniroma1.it

Abstract. The post-Newtonian parameter γ, unity in general relativity, controls the delay and the deflection of photons induced by the space-time curvature produced by any mass. A precise determination of this parameter can be attained exploiting the Shapiro time delay and the corresponding Doppler shift affecting the propagation of radio signals between a ground antenna and a spacecraft near a superior solar conjunction. In its cruise phase to Mercury (from October 2018 to December 2025), the spacecraft BepiColombo will experience eleven superior solar conjunctions, thus offering an excellent opportunity to test general relativity. The experiment will benefit from very accurate range and Doppler measurements, enabled by a multi-frequency radio link in X and Ka bands (8 and 34 GHz) and a high rate (24 Mcps) pseudo-noise ranging code. The multi-frequency link configuration allows the suppression of the plasma noise due to the solar corona. In this paper, we report the results of a comprehensive analysis based on the latest spacecraft trajectory and realistic numerical simulations. We find that γ can be determined with an accuracy of 5.7×10^{-6} with just one conjunction in July 2022, thus improving by a factor of 4 the result obtained by the Cassini mission in 2002. This accuracy can be further increased by selecting a limited number of favourable superior solar conjunctions, down to 2.2×10^{-6} when all of them are combined.

Keywords: General relativity, BepiColombo, Shapiro time delay, PPN parameters, Mercury, Experimental gravitation.

1. Introduction

The BepiColombo mission [1] is devoted to the exploration of Mercury, the innermost planet of the solar system. The mission, jointly developed by the European Space Agency (ESA) and the Japanese Aerospace eXploration Agency (JAXA), entails the release of two spacecraft in hermean orbit. The Mercury Magnetospheric Orbiter (MMO, built by JAXA), will be inserted into an elliptical polar orbit (590 x 11600 km altitude) to study the exosphere and the magnetosphere

of the planet. A low altitude and near circular polar orbit (480 x 1500 km) will allow the Mercury Planetary Orbiter (MPO, developed by ESA) to investigate the surface geology and the interior structure of the planet.

The Mercury Orbiter Radio science Experiment (MORE), hosted on the MPO, exploits advanced tracking instrumentation both onboard and on ground, enabling highly accurate range and Doppler measurements [2]. The use of a multi-frequency radio link in X and Ka bands will provide accuracies smaller than 3 micron/s (at 1000 seconds integration time) and 20 cm in range, at almost all solar elongation angles [3]. The MORE investigation is devoted to the determination of the gravity field and the rotational state of the planet from the Mercurycentric orbit of MPO (see e.g. [4]), and to carry out tests of General Relativity (GR) from the determination of the heliocentric motion of Mercury [5]. Thanks to the proximity to the Sun, the orbit of Mercury provides information on the fundamental structure of gravity. The GR tests of MORE will estimate, in a Parametrized formulation of the Post-Newtonian expansion of the metric (PPN, see e.g. [6]), the Eddington parameters β and γ, the preferred frame parameters α_1, α_2, and the Nordtvedt parameter η, which controls possible violations of the strong equivalence principle. The parameter γ has the peculiarity to affect not only the dynamics of a body, but also the propagation of radio-waves as a consequence of the space-time curvature. The effect is strongly magnified when the signal passes close to the Sun. Therefore, γ can be determined before the arrival at Mercury exploiting radio data collected when the spacecraft is close to a superior solar conjunction (as seen from the Earth).

Several superior conjunctions will occur during the cruise phase of BepiColombo. In this work we aim to analyze all conjunctions by means of a full set of numerical simulations, giving an assessment of the accuracies attainable in the determination of γ and identifying the main critical issues to be considered in the planning and execution of the experiment. The work is organized as follows: In Section 2 we introduce the physical principles of the experiment; In Section 3 we describe the characteristics of the BepiColombo cruise phase; Section 4 introduces the assumptions and the simulation scenario; In Section 5 we present and discuss the results; Conclusions are given in Section 6.

2. The solar conjunction experiment: from Cassini to BepiColombo

According to GR, the propagation of radio waves undergoes a delay and a deflection as a consequence of the space-time curvature. These effects are due to the space components of the metric and can be seen as a measure of the space curvature produced by a unit mass [7]. In the PPN expansion of the metric, the amount of space curvature produced by a mass is controlled by the parameter γ, whose value is unity in GR. The radio delay on a single leg signal, known as

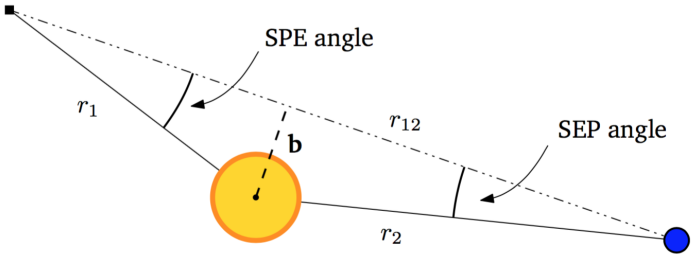

Figure 1. The geometry of a superior solar conjunction

Shapiro time delay [8], is:

$$\Delta t = \frac{(1+\gamma)Gm}{c^3} \ln\left(\frac{r_1 + r_2 + r_{12}}{r_1 + r_2 - r_{12}}\right), \tag{1}$$

where G is the gravitational constant, c the velocity of light and m the mass of the body producing the space-time curvature (e.g. the Sun); r_1, r_2 and r_{12} are respectively the positions of the transmitter and the receiver and their mutual distance expressed in a system whose origin is in the center of mass of the massive body. If the receiver, the curvature-generating body and the transmitter are nearly aligned (i.e. near a superior conjunction in our case), it follows that $r_1 + r_2 \approx r_{12}$, and the effect is enhanced. This phenomenon can be suitably used to test GR when a spacecraft is close to a Superior Solar Conjunction (SSC). In this geometric configuration radio waves sent toward the spacecraft and back to the ground station pass very close to the Sun surface and the Equation 1 can be approximated as [6]:

$$\Delta t = \frac{(1+\gamma)Gm_\odot}{c^3} \ln\left(\frac{4r_1 r_2}{b^2}\right), \tag{2}$$

where $b << r_1, r_2$ is called the impact parameter (see Figure 1). On the other hand, the signal experiences also a frequency shift given by:

$$\frac{d\Delta\nu}{\nu} = \frac{d\Delta t}{dt} = -2\frac{(1+\gamma)Gm_\odot}{c^3 b}\frac{db}{dt}. \tag{3}$$

Such a Solar Conjunction Experiment (SCE) was performed for the first time by the Cassini-Huygens mission in its cruise phase to the Saturn system. The data analysis of the June 2002 solar conjunction provided the estimate of $\gamma - 1 = (2.1 \pm 2.3) \times 10^{-5}$ by means of Doppler measurements only [9]. The effects in Equation 2 and Equation 3 directly impact on range and Doppler observables: the smaller the value of b, the larger the time delay and frequency shift will be. Note that the frequency shift depends also on the rate of change of the impact parameter. The larger db/dt is, the larger the frequency shift. "Fast" conjunctions offer better opportunities to test GR.

The use of the relativistic Doppler shift for testing GR during SSC was never used before Cassini for the reason that plasma noise due to the solar corona is very large when the beam passes very close to the Sun. Cassini overcame the problem by adopting a multi-frequency microwaves link at X and Ka bands (7.2 - 8.4 GHz and 34.0 - 32.5 GHz). The Cassini experiment was enabled by two dedicated onboard units in addition to the standard X band transponder used for telecommands and telemetry: a frequency translator capable of receiving an uplink at Ka band (34 GHz) and retransmitting it coherently (at 32.5 GHz), and a Ka band exciter providing a second Ka band signal coherent with the X band uplink. The supporting ground antenna (DSS 25 of NASA's Deep Space Network, located in Goldstone, California) was equipped with a Ka band transmitter and additional instrumentation for precise antenna pointing and for the calibration of tropospheric delays. However, the Cassini radio link did not support plasma free range measurements.

BepiColombo adopts the same link configuration as Cassini, with the addition of a precision ranging channel both a X and Ka band. In 2014, ESA has successfully tested Ka band transmit capabilities at its Deep Space Antenna DSA 3 in Malargue (Argentina), and is planning to reach full operational capabilities to support the MORE investigation, together with NASA's DSS 25 antenna. Thanks to these upgrades and the availability of data collected during several SSC, BepiColombo is expected to bring substantial improvements in the determination of γ.

Historically, tests on γ started using the deflection of light. Curiously, although the three effects (bending, delay, and frequency shift) are inherently related, only the bending was known to Einstein, while the associated delay was recognized as late as 1964 by I.I. Shapiro [6, Chapter 7]. Tests on bending of light have been done by using VLBI techniques, where the changes in the angular separation of signals from strong quasi-stellar radio source passing close to the Sun are inferred from time delay. The most recent analysis yielded $\gamma - 1 = (-0.8 \pm 1.2) \times 10^{-4}$ [10].

The Global Astrometric Interferometer for Astrophysics mission (GAIA) offers an exquisite opportunity to measure the deflection of light in the optical band. Launched in 2013 and currently operative in the Lagrangian point L_2, GAIA will observe the deflection of light from $> 10^6$ stars. The GAIA measurement will likely obtain an estimate of γ of about 2×10^{-6} [11]. The independent estimates of GAIA and BepiColombo will have about the same level of accuracy, thus providing a very reliable test of GR. A violation of GR found by both the missions would greatly increase the confidence in the result.

2.1. Plasma noise cancellation

The refractive index of dispersive media, such as plasmas, depends on the frequency of the radio signal. This dependence is exploited since a long time,

e.g. in GPS, to single out and remove the path delay and its derivative due to plasmas along the propagation path (in our case solar corona, interplanetary plasma and ionosphere). Indeed, by a suitable selection of the link configuration and in the limit of geometric optics, plasma noise can be completely canceled out in both Doppler and range observables.

Following the treatment in [12], we consider a two-way, coherent radio-link, with uplink and downlink frequencies f_U and $f_D = \alpha f_U$, where α is the transponding ratio of the onboard transponder. Neglecting incoherent noise (such as thermal noise of the receiver), the generic radio observable y (e.g. Doppler or range) is the sum of a non-dispersive contribution y_t and contributors coming from the path delay in the uplink and downlink:

$$y = y_t + \frac{P_U}{f_U^2} + \frac{P_D}{f_D^2} = y_t + \frac{P_U}{f_U^2} + \frac{P_D}{\alpha^2 f_U^2}\,. \tag{4}$$

The quantities P_U and P_D are proportional to the total electron content (electrons/m^2) or its derivative, scaled with the square of the uplink and downlink carrier frequencies. In Equation 4, the plasma-free observable y_t, along with P_U and P_D, are unknown. The multi-frequency plasma removal scheme exploits the three links (X/X, Ka/Ka and X/Ka) and the related observables to solve for the three unknowns in the linear system

$$\begin{aligned} y_{kk} &= y_t + \frac{P_U}{f_{Ukk}^2} + \frac{P_D}{\alpha_{kk}^2 f_{Dkk}^2} \\ y_{xk} &= y_t + \frac{P_U}{f_{Uxk}^2} + \frac{P_D}{\alpha_{xk}^2 f_{Dxk}^2} \\ y_{xx} &= y_t + \frac{P_U}{f_{Uxx}^2} + \frac{P_D}{\alpha_{xx}^2 f_{Dxx}^2}\,. \end{aligned} \tag{5}$$

For BepiColombo α_{kk} = 3360/3599, α_{xk} = 3344/749 and α_{xx} = 880/749, as recommended by the regulations from the International Telecommunications Union. The linear system in Equation 5 provides the plasma-free observable y_t, together with the ancillary quantities P_U and P_D.

Such a calibration scheme removes plasma noise at nearly all solar elongation angles. Its effectiveness was demonstrated during the Cassini SCE. However, as explained in [13], when the impact parameter becomes too small (few solar radii), diffraction effects due to physical optics may cause occasional signal fading, especially at X band. Moreover, density gradients in the solar corona and magnetic corrections to the refractive index cannot be neglected when the beam passes very close to the Sun (2-3 solar radii). The value of b at which the cancellation scheme becomes ineffective is not predictable, as it depends on the level of solar activity. The analysis of the link frequency stability during Cassini SCE shows

that only during one tracking pass, at $b < 5R_\odot$, the cancellation scheme failed. The frequency stability of the link (measured in terms of Allan deviation at 1000 seconds integration time) was always around 10^{-14} when $b > 7R_\odot$ [14].

3. The cruise phase of BepiColombo

In the latest mission scenario that has been provided, the launch window for the Mercury Composite Spacecraft (MCS, including MPO, MMO, solar panels and the solar-electric propulsion module) opens on 16 October 2018 and lasts 31 days. The launch is scheduled from the Centre Spatial Guyanais located in Kourou (French Guiana) by means of a dedicated Ariane 5 launch vehicle. The detailed description of the BepiColombo cruise phase is given in [15]: after 18 months from launch, the spacecraft returns to Earth and is deflected toward Venus, performing two flybys of the planet and reducing the perihelion to the orbit of Mercury. Afterward, six Mercury flybys decrease the relative velocity down to 1.85 km/s. The use of the onboard propulsion system will further reduce the relative velocity in order to enable a weak capture of the spacecraft by Mercury in December 2025, without the need of an orbit insertion maneuver. The scientific operations of MPO start in March 2026, after several maneuvers aiming to place the spacecraft in its nominal orbit around the planet. An overview of the cruise phase‡, projected into the Ecliptic plane of J2000, is reported in Figure 2. Dates, altitudes and relative velocities of the flybys are given in Table 1.

Reaching Mercury is a challenging task, as it requires a large decrease of the spacecraft mechanical energy. The strategy adopted for BepiColombo exploits a combination of Solar-Electric Propulsion System (SEPS) and planetary flybys. The SEPS thrust performances depend on the heliocentric distance, with a maximum value of 290 mN [16]. The activation of SEPS is an output of the trajectory optimisation: the current schedule involves thrusted phases for about 600 days, or $\approx 23\%$ of the entire cruise time (see Figure 3).

Referring to Figure 1, solar conjunctions are characterized by small values of the Sun-Earth-Proble (SEP) angle, while for an object in the inner solar system, the Sun-Probe-Earth (SPE) angle discriminates among superior conjunctions (SPE near 0 degrees) and inferior conjunctions (SPE near 180 degrees). The behaviour of the SPE angle is plotted in Figure 3, along with markers indicating planetary flybys and thrusted arcs. There are eleven SSC during the journey of BepiColombo to Mercury, and each one is an opportunity to test GR. The main characteristics of the SSCs are reported in Table 2. Note that the spacecraft will never be occulted behind the solar disk ($b < R_\odot$). The minimum value of the impact parameter is $b = 1.16R_\odot$, reached during the SSC #7 in May 2024. db/dt reaches the maximum

‡ The SPICE kernel of the cruise trajectory adopted for the analysis is available on the website http://radioscience.dima.uniroma1.it/publications.php

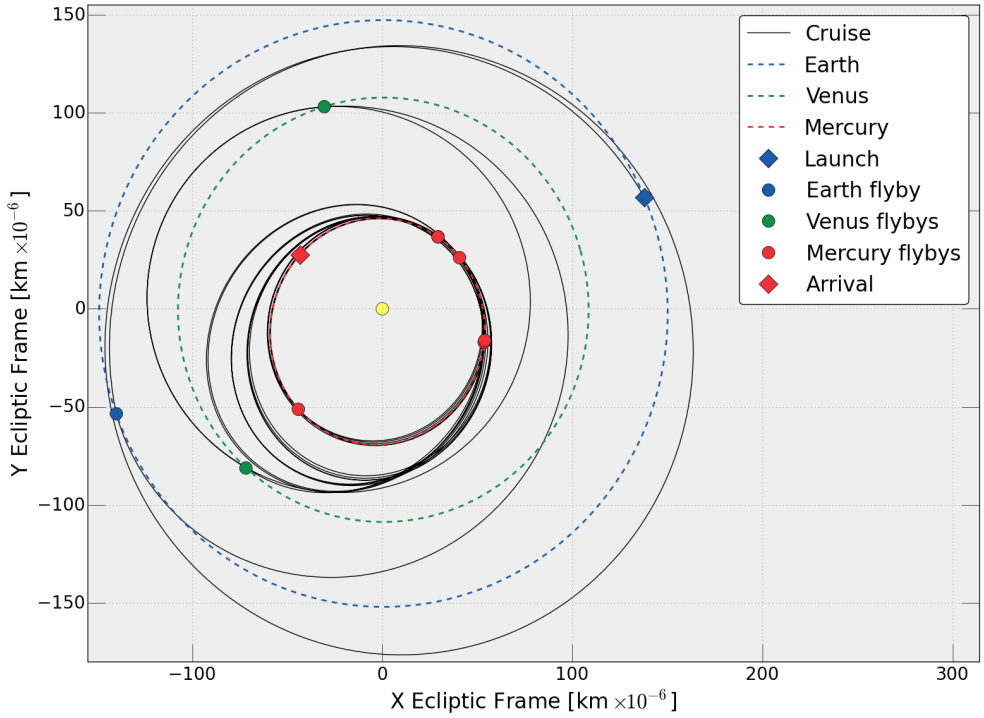

Figure 2. The cruise phase of BepiColombo, projected on the Ecliptic plane

value in this conjunction ($3.93R_\odot$/day). For comparison, the Cassini SCE in June 2002 was characterized by $b_{min} = 1.6R_\odot$ and $db/dt_{max} = 3.7R_\odot$/day.

4. Assumptions and simulation setup

Although tests of relativistic gravity are one of the main goals of BepiColombo, which ones and how many SSCs are going to be exploited is not yet defined.

Table 1. Date, altitude and relative velocity of the planetary flybys of BepiColombo.

Planetary flyby	**Date**	**Altitude** [km]	**Velocity** [km/s]
Earth	10 Apr 2020	11708	4.01
Venus 1	15 Oct 2020	10576	7.98
Venus 2	11 Aug 2021	1041	8.08
Mercury 1	02 Oct 2021	221	6.55
Mercury 2	23 Jun 2022	102	6.35
Mercury 3	20 Jun 2023	205	3.64
Mercury 4	05 Sep 2024	354	2.93
Mercury 5	02 Dec 2024	39997	2.68
Mercury 6	09 Jan 2025	299	1.84

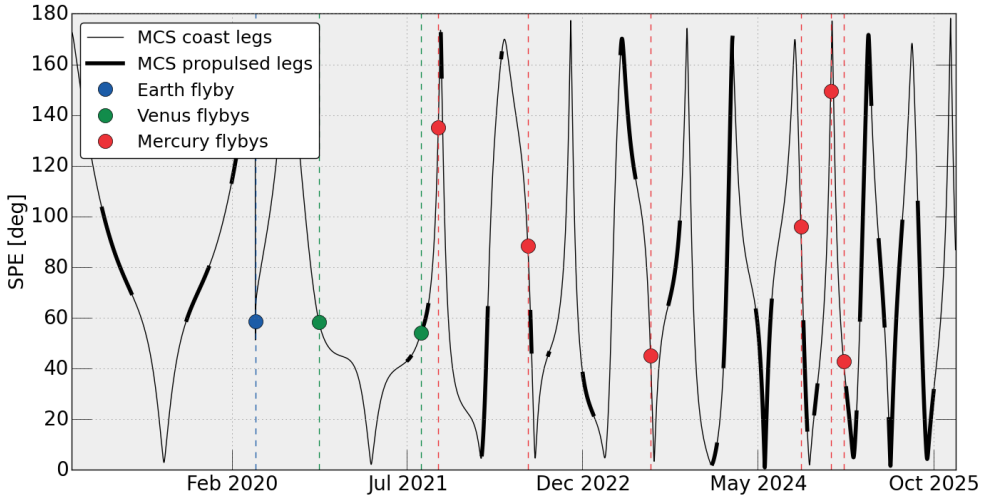

Figure 3. The Sun-Probe-Earth (SPE) angle during BepiColombo's cruise phase. Superior solar conjunctions occur when SPE $\approx 0°$. SPE $\approx 180°$indicates an inferior conjunction. Note that the first event when SPE is $\approx 0°$is actually an inferior conjunction, as MCS is temporarily in the outer solar system. Thick lines represent the periods when solar electric propulsion activation is planned.

Our purpose is to assess the level of accuracy attainable in the determination of γ for each SSC and their combination, searching for best estimation strategies and emphasizing the critical aspects of the experiment.

Table 2. Date, minimum impact parameter b and maximum rate db/dt of the 11 superior solar conjunctions in the cruise phase of BepiColombo.

SSC	Date	$\mathbf{b}_{min}$ [$R_\odot$]	$\mathbf{db/dt}_{max}$ [$R_\odot$/day]
#1	18 Mar 2021	4.28	1.97
#2	05 Feb 2022	7.52	2.21
#3	14 Jul 2022	5.93	3.54
#4	05 Feb 2023	8.02	1.90
#5	30 Jun 2023	3.99	3.90
#6	16 Dec 2023	4.62	0.27
#7	21 May 2024	1.16	3.93
#8	30 Sep 2024	2.88	2.11
#9	07 Feb 2025	7.41	2.02
#10	27 May 2025	1.88	3.58
#11	12 Sep 2025	6.21	2.35

4.1. Higher PN order corrections

Equation 1 holds to PN order 1 corrections in the small parameters v^2/c^2 and $Gm/(c^2 r)$. We shall discuss if higher order are required given the extremely accurate radio observables of MORE. Corrections to PN order 1.5, due to the motion of the Sun, are discussed in [17, 18]. As demonstrated in [19], they are negligible for the MORE investigation. On the other hand, second order corrections in the Shapiro formula, due to the bending of light path, may become relevant in case of small impact parameters. Moyer [21], proposed a simple correction to Equation 1 to account also for PN second order terms:

$$\Delta t = \frac{(1+\gamma)Gm}{c^3} \ln \left[\frac{r_1 + r_2 + r_{12} + \dfrac{Gm(1+\gamma)}{c^2}}{r_1 + r_2 - r_{12} + \dfrac{Gm(1+\gamma)}{c^2}} \right]. \tag{6}$$

A precise formulation for the light time function including PN order 2 effects can be found in [18, 20]. However, [18] shows that Equation 6 is a good approximation to the exact solution for all practical cases. Figure 4 shows the effect on the radio observables due to the Shapiro time delay compared with the additional 2-PN corrections. For its extreme characteristics, we consider the case of SSC #7. If plasma-free observations were available when b is below few solar radii ($\approx 4R_\odot$), second orders corrections, which may reach tens of cm, shall be taken into account.

4.2. Assumptions and simulation scenario

We assume a one month long experiment around each SSC. In this period both Goldstone and Malargue ground antennas are supposed to provide plasma-free range and Doppler observables, corrected also for tropospheric path delays by means of an advanced media calibration system based on water vapour radiometers, as in Cassini's experiment. Because of the small separation in longitude between the two ground stations (about 45 degrees), their daily tracking periods overlap. Only Malargue data are retained in the overlapping time. As discussed in Section 2.1, numerical simulations must take into account that, when the signal path is close to the Sun, the X-band link enters in the strong scintillation regime, where phase measurements become unreliable and the plasma noise removal scheme cannot be applied. Even if in practice the data would gradually degrade as the SPE angle decreases (see e.g. [22]), we adopt a a simpler approach and assume a perfect plasma noise removal till a selected, realistic minimum value of b, discarding all data collected below this limit. We assume as nominal value for the impact parameter threshold $b_t = 7R_\odot$, a likely value inferred from the analysis of Cassini Doppler data. Since this cutoff has important consequences on the estimate of γ, we also carried out a sensitivity analysis by varying this value.

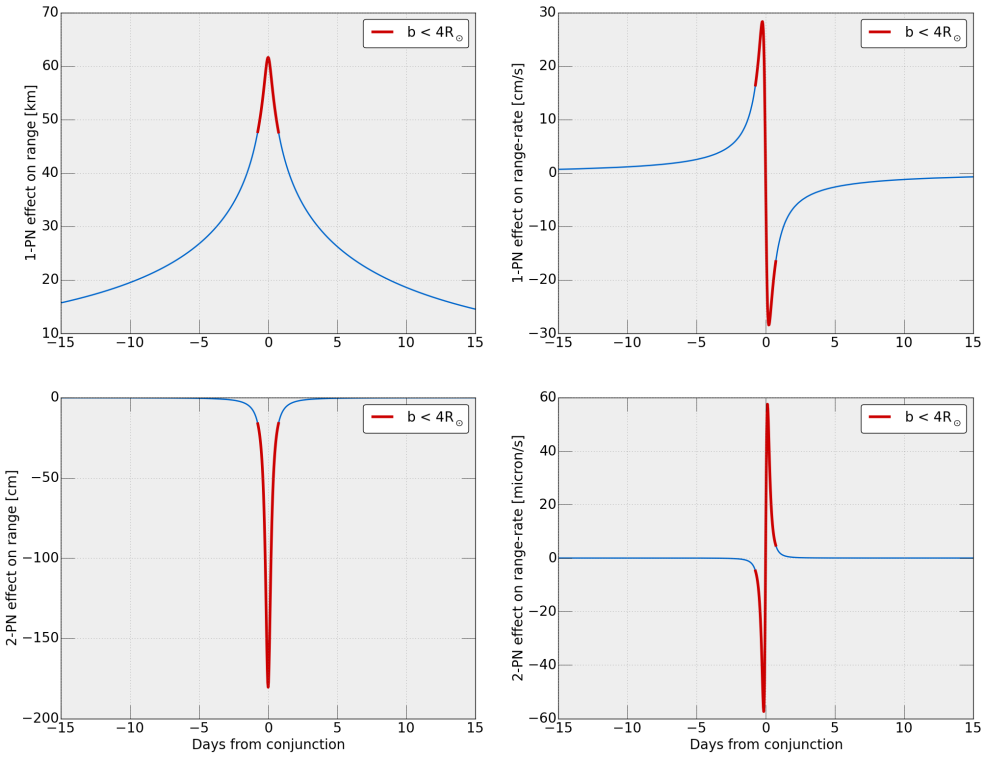

Figure 4. Expected relativistic signatures on two-way range and range-rate during the SSC #7 in May 2024 ($\gamma = 1$). The top panel shows the PN order 1 effects. Second order effects (PN order 2) as given in Equation 6, are shown in the bottom panel. The reference date of each conjunction corresponds to the minimum value of the impact parameter b (see Figure 1).

As BepiColombo uses SEPS over large segments of the cruise, not all SSC could be exploited for a test of GR. Indeed, a good estimate of γ requires a quiet spacecraft, where non-gravitational accelerations are minimized or constant. As illustrated in Figure 3, many SSC include thrust legs. In our analysis, aimed at assessing the ultimate limits of BepiColombo GR tests, we assume that all SSCs are taking place during coast arcs. Moreover, to further optimize the experiment, we assume that the spacecraft elements, in particular the large solar panels needed by SEPS, are oriented toward the Sun at constant aspect angle. This spatial orientation is compatible with the flight rules and can be maintained with an accuracy of fractions of a degree. The direction of the acceleration, constant in the body frame, is therefore always radially oriented with respect to the Sun§. Although in principle the non-gravitational accelerations of the spacecraft are measured by a high accuracy onboard accelerometer (the Italian Spring Accelerometer, ISA, [23]), the characteristic frequencies of the relativistic signals (10^{-6} - 10^{-5} Hz) are outside the main sensitivity band of the instrument (10^{-4} - 10^{-1} Hz). Moreover,

§ Only the high gain antenna (1 m diameter) will be necessarily pointed toward the Earth. The small variation of the sun aspect angle across conjunction can be modeled to a large extent.

the characteristics of the accelerometer at long time scales are poorly known, as they are very difficult to assess from ground tests. In turn, the extensive range and Doppler tracking of the spacecraft may be used to characterize the behaviour of the accelerometer in the low frequency regime, by comparing the estimate of the non-gravitational accelerations with the ISA readings. Lastly, the parameters estimate is based on a classical non-linear least squares method (see e.g. [24, 25]).

The simulation scenario, as described above, is hereafter summarized:

- DSS 25 Goldstone and DSA 3 Malargue track with MCS providing Doppler and range plasma-free observables;
- Doppler and range are simulated respectively every 60 and 300 seconds, with white noise of 12.25×10^{-4} cm/s and 30 cm¶;
- data collected below a threshold value of b_t (nominally $b_t = 7R_\odot$) are discarded;
- 30 days of observations around the epoch of minimum b;
- all SSC are assumed to be thrust-free;
- non-gravitational accelerations are modeled by means of diffuse and specular reflectivity of spacecraft elements.

The solve-for parameters list includes:

- the heliocentric state vector of MCS at the beginning of the one month observation window;
- the PPN parameter γ, whose effect is computed from Equation 6;
- the solar radiation pressure acceleration through a scale factor coefficient.

Furthermore, for the parameter γ we adopt an *a priori* uncertainty of $\sigma_\gamma = 6.9 \times 10^{-5}$, three times larger than the Cassini estimate.

4.3. Planetary flybys during conjunctions

Superior conjunctions including a planetary flyby in the selected observation window need further considerations, as the proximity of a massive body complicates the dynamics of the spacecraft. This situation occurs in June 2023, when the second Mercury flyby happens about seven days before SSC #5. For this conjunction, uncertainties in the planet's ephemeris and gravity field need to be accounted for in the analysis. Failing to do so may lead to unrealistically small covariances.

¶ According to Gaussian statistics, the standard deviation can be rescaled at different integration times. These values are equivalent to an Allan deviation of 10^{-14} at 1000 seconds for Doppler and the acquisition of one range measurement with an accuracy of 20 cm every 10 minutes (a realistic assumption).

Following the scenario summarized in Section 4.2, the orbital arc after the closest approach to the planet would be strongly constrained by the flyby event itself. Indeed, making the assumption that the gravity field and the ephemeris of Mercury are perfectly known would result in small formal errors in the initial state vector of the spacecraft (heliocentric position and velocity at the beginning of the thirty days arc). The small state covariance is a consequence of the strong sensitivity of the outbound trajectory on the (pre-flyby) initial conditions. Indeed, the accurate tracking data in the outbound arc strongly constrain the inbound trajectory. This very accurate determination of the state vector would result also in a very accurate determination of γ. In reality, although the MESSENGER mission largely improved the knowledge of the gravity field and the ephemeris of Mercury [26], the residual uncertainties may be still sufficient to induce large errors in the spacecraft state propagation after the closest approach. This is especially true for the ephemeris, whose errors will be certainly larger than during the MESSENGER mission, when observations were available. For these reasons, the unrealistic constraint in the trajectory could easily result in a biased estimate of γ.

In order to address these problems, we considered three different strategies:

(i) Follow the standard assumptions given in Section 4.2, but using a "wrong" hermean ephemeris and gravity field in the fit, different from those used in the data generation stage. The references ephemeris are the JPL DE430 and DE432 [27, 28], which include some MESSENGER data. Uncertainties in the gravity field are provided in [26];

(ii) Use the assumptions of case (i), but including Mercury's state vector in the global solution;

(iii) assume the epoch state just after the flyby, at the penalty of a shorter data arc.

5. Results

The results of the simulations are summarized in Table 3. All conjunctions, with the exception of SSC #6, result in improvements of the Cassini determination, with estimates of γ at a level of 10^{-5} or below.

For SSC #5, occurring near planetary flybys, we verified that the approach (i) described in Section 4.3 results in the smallest formal uncertainty for γ: 3.0×10^{-6}. However, this values is illusory, since the spurious signal due to the imperfect knowledge of Mercury's orbit is, as expected, quite large (several tens of km and cm/s in the outbound trajectory) resulting in a biased estimate. Including at least the ephemeris of the planet in the set of solve-for parameters, as in the scenario (ii), Section 4.3, is mandatory. The gravity field uncertainties turned up to be a minor issue. In approach (ii) the formal accuracy is larger (6.0×10^{-6}) and the solution is unbiased. Lastly, with the more conservative approach (iii), we obtain a result comparable with that from case (ii) (see Table 3). We will consider only

Table 3. Formal uncertainty in the estimate of the PPN parameter γ for the 12 BepiColombo superior solar conjunctions in the cruise phase, assuming that plasma-free data are available down to $b_t = 7R_\odot$. For conjunction #5, which includes a Mercury flyby in the observation window, the results correspond to the three solution strategies described in Section 4.3.

SSC	Formal γ [$\times 10^6$]	SSC	Formal γ [$\times 10^6$]
#1	8.3	**#7**	6.2
#2	8.3	**#8**	7.4
#3	5.7	**#9**	6.8
#4	10.0	**#10**	5.3
#5	(i) 3.0** (ii) 6.0 (iii) 6.4	**#11**	6.8
#6	31.4		

**Not realistic, see Section 5

this strategy (iii) from now on.

The attainable accuracies for γ vary by just a factor of two between the various conjunctions except SSC #6. The best opportunities are found in July 2022 and May 2024 (with SSC #3 and #10) with an estimate of γ at level of 5.5×10^{-6}. According to the current mission profile, SSC #10 is included in a thrusted arc for a large fraction of the time (see Figure 3). At this time it is not known whether this opportunity can be exploited.

5.1. Sensitivity to the plasma noise calibration scheme

In order to increase the accuracy of the test, it is desirable to minimize the impact parameter b. On the other hand, as discussed in Section 2.1, the plasma cancellation scheme is inapplicable when the X band signal enters in the strong scintillation regime. It is therefore essential to assess the sensitivity of the test as a function of the cutoff value of the impact parameter. For each of the SSC, we have determined the estimation accuracy of γ as a function of the threshold impact parameter b_t for the applicability of the plasma noise cancellation procedure. The results are shown in Figure 5. SSC #1 shows the larger sensitivity to b_t. It provides good results if small values of b_t can be attained. At the same time a fast degradation is found as b_t increases. SSC #3, #5, #7, #8, and #10 appear to be very good opportunities, as the estimation accuracies would not be strongly degraded even for large b_t (strong solar activity), and there would be substantial improvements if the coronal environment is favourable. Particularly promising is SSC #7 in May 2024, which still provides an accuracy of 6.4×10^{-6} for $b_t = 9R_\odot$ and significantly better results in case of low value of b_t. However, both SSC #7 and #10 would require a change in the thrust profile. SSC #11 is less attractive if compared to those mentioned above, while SSC #2, #4 and #9 are characterized

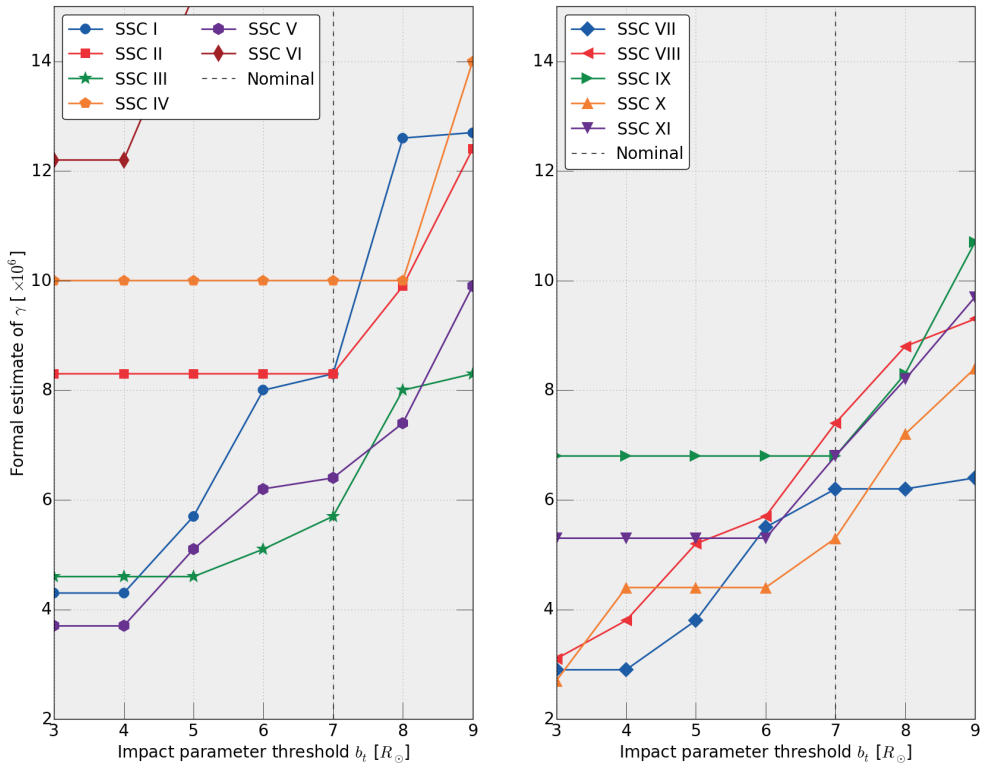

Figure 5. Formal uncertainty in the estimate of γ for each conjunction as a function of cutoff impact parameter b. b_t is the minimum distance of the radio beam from the Sun at which the multi-frequency plasma cancellations scheme can be used. When $b < b_t$, the X band signal enters in the strong scintillation regime, preventing reliable phase measurements.

by a minimum impact parameter $> 7R_\odot$, and therefore would not benefit from a lower b_t. Lastly, SSC #6 would result in an improvement over the Cassini estimate only if the corona environment is favorable.

5.2. Combination of different conjunctions

The accuracy of the test can be substantially improved by combining data from two or more SSC in a multi-arc approach (see e.g. [24, Chapter 5]). We have determined the best attainable accuracy with a combined solution and ranked different combinations. Together with the sensitivity analysis, this is important in order to guide the decisions of the BepiColombo project, should a change in the thrust profile be considered. The results are reported in Table 4. The best attainable estimate in the nominal scenario, when all the SSC are combined, is 2.2×10^{-6}. However the combination of all thrust-free arcs¶ would result in just a 50% degradation of the estimation accuracy, or 3.2×10^{-6}. When only the best opportunities (SSC #3 and #10), are combined, the accuracy becomes 3.9×10^{-6}.

¶ To simplify, we considered SSC when SEPS is scheduled to be used < 30% of the observation window, i.e. SSC #1, #3, #4, #5 and #8.

Table 4. Formal uncertainty in the estimate of γ ($\times 10^6$) for a multi-arc solution including different combination, tracking assumptions and plasma-free data availability. Thrust-free conjunctions are #1, #3, #4, #5 and #8.

	#3 + #10	**Thrust-free**	**All**
Nominal tracking + $\mathbf{b}_t = 7R_\odot$	3.9	3.2	2.2
h24 tracking + $\mathbf{b}_t = 7R_\odot$	2.8	2.3	1.5
h24 tracking + $\mathbf{b}_t = 5R_\odot$	2.1	1.7	1.2

5.3. Contingency scenarios

We also investigated the effect of some deviations from the nominal tracking scenario described in Section 4.2. We considered the following cases:

- Estimate based on Doppler data only;
- Estimate based on range data only;
- Around the clock tracking;
- Use of only one ground antenna;
- Reduction of the tracking period to 20, 15 and 10 days.

As a reference case, we examine SSC #3, which provides a nominal estimate of 5.7×10^{-6}. The results of the simulations are shown in Table 5. We note that Doppler and range data are almost equivalent, although range provides slightly better results. This is not surprising, as the characteristics time scales of the relativistic signal is comparable to the integration time at which the errors in integrated Doppler and differenced range become approximately equivalent ($\approx$ 15 hours in the case of MORE).

We verified the importance of having at least two ground stations with Ka uplink capabilities. Because of the small distance in longitude and the fact that SSC #3 takes place in July, an experiment based only on Goldstone data (i.e. with an antenna located in the boreal hemisphere) provides most of the information. The opposite is true for a SSC occurring in the boreal winter. We simulated a scenario where ground antennas could support around the clock tracking. This scenario requires at least one additional ground station with Ka band capabilities at the appropriate longitudes (for example in Japan[+] or Australia). The upgrade of one antenna to full Ka band capabilities at each DSN site is currently being considered by NASA to support future planetary missions. Continuous coverage would lead to a significant improvement of the test (about 30%). In an extreme scenario, if around the clock tracking is used in favourable conditions of the coronal environment ($b_t = 5R_\odot$), and data of all SSC are combined, the ultimate accuracy of the test would be 1.2×10^{-6} (see Table 4).

[+] A new 34 meters antenna is being built in Japan, also in view of MMO tracking. In principle it could be upgraded to Ka uplink.

Table 5. Formal uncertainty in the estimate of γ in solar conjunction #3 (July 2022), assuming observation scenarios different from the one described in Section 4.2. The reference scenario yield the estimate $\sigma_\gamma = 5.7 \times 10^{-6}$.

	Formal γ [$\times 10^6$]		**Formal γ [$\times 10^6$]**
only Malargue	8.2	**only Goldstone**	5.9
Doppler only	10.7	**20 days only**	8.0
range only	7.3	**15 days only**	10.2
h24 tracking	4.1	**10 days only**	22.3

The degradation in the accuracy from a shorter tracking period is another important indication obtained from our analysis. Reducing the ground antenna coverage to 20, 15 and 10 days produce respectively about a 40%, 80% and 300% decrease in the estimation accuracy of γ. In order to attain a significant improvement over the Cassini test, the tracking period shall not be lower than 20 days.

5.4. Non-gravitational accelerations

The estimate of the scale factor for the solar radiation pressure indicates that non-gravitational accelerations are inferred with an accuracy lower than 3×10^{-9} cm/s^2 for all the SSC. This is about one order of magnitude lower than the level of accuracy in the Cassini estimate of the non-gravitational accelerations (mainly due to anisotropic emission from radioisotope thermoelectric generator radiation [14]).

6. Conclusions

We have analyzed the superior solar conjunctions of the BepiColombo spacecraft during the seven years and two months cruise phase to Mercury, addressing the main critical issues of experiments aiming at a determination of the Post-Newtonian parameter γ. We presented a full set of numerical simulations under different assumptions for tracking coverage and availability of plasma noise calibrations, giving an assessment of the attainable accuracies in each conjunction. All simulations are based upon the latest available trajectory, for a launch in October 2018. We find that all but one conjunctions will provide a substantial improvement of the Cassini results $\gamma - 1 = (2.1 \pm 2.3) \times 10^{-5}$. The simulations show that in an optimal configuration, γ may be determined at level of 5.5×10^{-6} with just one conjunction (SSC #3 in July 2022). Further improvements can be attained by combining data from multiple conjunctions. We find a limit accuracy of 2.2×10^{-6} when data from all conjunctions are exploited.

It should be noted that the launch date and the reference trajectory of the mission has changed many times over the past years. Further changes may be expected. This work is intended to identify the critical elements of the experiments, which are likely to be largely independent from the actual trajectory. Indeed, in [29] is studied the BepiColombo SCE in cruise considering the older launch date in July 2017, arriving to similar results and conclusions. Our results and indications will be updated once BepiColombo is launched.

References

[1] Benkhoff, J., Casteren, J.V., Hayakawa, H., Fujimoto, M., H., Laakso, Novara, M., Ferri, P., Middleton, H.R., and Ziethe, R. "BepiColombo-Comprehensive exploration of Mercury: Mission overview and science goals". In: *Planetary and Space Science* 58.1-2 (2010). Comprehensive Science Investigations of Mercury: The scientific goals of the joint ESA/JAXA mission BepiColombo, pp. 2–20. ISSN: 0032-0633. URL: http://www.sciencedirect.com/science/article/pii/S0032063309002840.

[2] Iess, L. and Boscagli, G. "Advanced radio science instrumentation for the mission BepiColombo to Mercury". In: *Planetary and Space Science* 49.14-15 (2001), pp. 1597–1608. ISSN: 0032-0633. URL: http://www.sciencedirect.com/science/article/pii/S0032063301000964.

[3] Iess, L., Asmar, S., and Tortora, P. "MORE: An advanced tracking experiment for the exploration of Mercury with the mission BepiColombo". In: *Acta Astronautica* 65.5-6 (2009), pp. 666–675. URL: http://www.sciencedirect.com/science/article/pii/S0094576509000356.

[4] Cicalò, S., Schettino, G., Di Ruzza, S., Alessi, E.M., Tommei, G., and Milani, A. "The BepiColombo MORE gravimetry and rotation experiments with the ORBIT14 software". In: *Monthly Notices of the Royal Astronomical Society* 457.2 (2016). DOI: 10.1093/mnras/stw052.

[5] Milani, A., Vokrouhlický, D., Villani, D., Bonanno, C., and Rossi, A. "Testing general relativity with the BepiColombo radio science experiment". In: *Phys. Rev. D* 66 (8 Oct. 2002), p. 082001. DOI: 10.1103/PhysRevD.66.082001.

[6] Will, C. M. *Theory and Experiment in Gravitational Physics*. Revised. Cambridge University Press, Mar. 1993. ISBN: 0521439736.

[7] Misner, C.W., Thorne, K.S., and Wheeler, J.A. *Gravitation*. Gravitation pt. 3. W. H. Freeman, 1973. ISBN: 9780716703440.

[8] Shapiro, I. I. "Fourth Test of General Relativity". In: *Phys. Rev. Lett.* 13 (26 Dec. 1964), pp. 789–791. DOI: 10.1103/PhysRevLett.13.789.

[9] Bertotti, B., Iess, L., and Tortora, P. "A test of general relativity using radio links with the Cassini spacecraft". In: *Nature* 425 (2003), pp. 374–376. DOI: 10.1038/nature01997.

[10] Lambert, S. B. and Le Poncin-Lafitte, C. "Improved determination of γ by VLBI". In: *Astronomy and Astrophysics* 529, A70 (May 2011), A70. DOI: 10.1051/0004-6361/201016370.

[11] Mignard, F. and Klioner, S. A. "Gaia: Relativistic modelling and testing". In: *Relativity in Fundamental Astronomy: Dynamics, Reference Frames, and Data Analysis*. Vol. 5. Proceedings of the International Astronomical Union. Apr. 2009, pp. 306–314. DOI: 10.1017/S174392130999055X.

[12] Mariotti, G. and Tortora, P. "Experimental validation of a dual uplink multifrequency dispersive noise calibration scheme for Deep Space tracking". In: *Radio Science* 48.2 (2013), pp. 111–117. ISSN: 1944-799X. DOI: 10.1002/rds.20024.

[13] Tortora, P., Iess, L., and Ekelund, J. E. "Accurate Navigation of Deep Space Probes using Multifrequency Links: the Cassini Breakthrough during Solar Conjunction Experiments". In: *IAF abstracts, 34th COSPAR Scientific Assembly*. Jan. 2002.

[14] Tortora, P., Iess, L., Bordi, J. J., Ekelund, J. E., and Roth, D. C. "Precise Cassini Navigation During Solar Conjunctions Through Multifrequency Plasma Calibrations". In: *Journal of Guidance Control Dynamics* 27 (Mar. 2004), pp. 251–257. DOI: 10.2514/1.997.

[15] Jehn, R. *BepiColombo Mercury Cornerstone Mission Analysis: The October 2018 Launch Option*. MAS Working Paper No. 609, BC-ESC-RP-500014, Issue 2.0. Robert-Bosh-Str. 5, 64293 Darmstadt, Germany: European Space Operation Center, ESOC, 2016.

[16] Striedter, F. *MTM Power and Thrust Model for Mission Analysis*. BC-ASD-TN-00209, Issue 6. Airbus Defense & Space, 2015.

[17] Will, C. M. "Propagation Speed of Gravity and the Relativistic Time Delay". In: *The Astrophysical Journal* 590.2 (2003), p. 683. URL: http://stacks.iop.org/0004-637X/590/i=2/a=683.

[18] Ashby, N. and Bertotti, B. "Accurate light-time correction due to a gravitating mass". In: *Classical and Quantum Gravity* 27.14 (2010), p. 145013. URL: http://stacks.iop.org/0264-9381/27/i=14/a=145013.

[19] Milani, A., Tommei, G., Vokrouhlický, D., Latorre, E., and Cicalò, S. "Relativistic models for the BepiColombo radioscience experiment". In: *Relativity in Fundamental Astronomy: Dynamics, Reference Frames, and Data Analysis*. Ed. by Klioner, S. A., Seidelmann, P. K., and Soffel, M. H. Vol. 261. IAU Symposium. Jan. 2010, pp. 356–365. DOI: 10.1017/S1743921309990652.

[20] Teyssandier, P. and Le Poncin-Lafitte, C. "General post-Minkowskian expansion of time transfer functions". In: *Classical and Quantum Gravity* 25.14 (2008), p. 145020. URL: http://stacks.iop.org/0264-9381/25/i=14/a=145020.

[21] Moyer, T. D. *Formulation for Observed and Computed Values of Deep Space Network Data Types for Navigation*. JPL Deep-Space Communications and Navigation Series. Wiley, 2005. ISBN: 9780471726173.

[22] Iess, L., Di Benedetto, M., James, N., Mercolino, M., Simone, L., and Tortora, P. "Astra: Interdisciplinary study on enhancement of the end-to-end accuracy for spacecraft tracking techniques". In: *Acta Astronautica* 94.2 (2014), pp. 699–707. ISSN: 0094-5765. URL: http://www.sciencedirect.com/science/article/pii/S0094576513002014.

[23] Iafolla, V., Fiorenza, E., Lefevre, C., Morbidini, A., Nozzle, S., Peron, R., Persichini, M., Reale, A., and Santoli, F. "Italian Spring Sccelerometer (ISA): A fundamental support to BepiColombo Radio Science Experiments". In: *Planetary and Space Science* 58.1-2 (2010), pp. 300–308. ISSN: 0032-0633. URL: http://www.sciencedirect.com/science/article/pii/S0032063309001019.

[24] Milani, A. and Gronchi, G. *Theory of Orbit Determination*. Cambridge University Press, 2010. ISBN: 9780521873895.

[25] Tapley, B., Schutz, B., and Born, G.H. *Statistical Orbit Determination*. Elsevier Science, 2004. ISBN: 9780080541730.

[26] Mazarico, E., Genova, A., Goossens, S., Lemoine, F. G., Neumann, G. A., Zuber, M. T., Smith, D. E., and Solomon, S. C. "The gravity field, orientation, and ephemeris of Mercury from MESSENGER observations after three years in orbit". In: *Journal of Geophysical Research: Planets* 119.12 (2014), pp. 2417–2436. ISSN: 2169-9100. DOI: 10.1002/2014JE004675.

[27] Folkner, W. M., Williams, J. G., Boggs, D. H., Park, R. S., and Kuchynka, P. "The Planetary and Lunar Ephemerides DE430 and DE431". In: *Interplanetary Network Progress Report* 196 (Feb. 2014), pp. 1–81.

[28] Folkner, W. M. *Planetary ephemeris DE432*. Jet Propulsion Laboratory, California. 2014. URL: http://naif.jpl.nasa.gov/pub/naif/generic_kernels/spk/planets/de432.pdf.

[29] Imperi, L. and Iess, L. "Testing general relativity during the cruise phase of the BepiColombo mission to Mercury". In: *Metrology for Aerospace (MetroAeroSpace), 2015 IEEE*. June 2015, pp. 135–140. DOI: 10.1109/MetroAeroSpace.2015.7180641.